Contents

1 Introduction **2**

2 Literature Review **3**

2.1 Current clinical diagnostic approaches . . . 3

2.2 Wearable technology . . . 3

2.3 Related Works . . . 3

2.3.1 Sensorised Gloves . . . 3

2.3.2 3D graphics in medical field . . . 4

3 Methodology **4**

3.1 Scenario setup and the general structure of the system . . . 4

3.2 Input Hardware . . . 5

3.3 Data acquisition . . . 6

3.3.1 Reading the input data . . . 6

3.3.2 Synchronisation . . . 6

3.3.3 Offline simulation . . . 7

3.4 Data Processing . . . 7

3.4.1 Coordinates . . . 7

3.4.2 Quaternion and Euler angle . . . 7

3.4.3 Stress and Strain . . . 8

3.4.4 Triggering . . . 8

3.4.5 Moving Average . . . 9

3.4.6 Locating Region . . . 10

3.5 Experiment with phantoms . . . 10

4 Results **11**

4.1 3D-Graphics . . . 11

4.2 2D-Graphics . . . 11

4.2.1 Stress plot . . . 11

4.2.2 Stress-Strain Plot . . . 12

4.3 Offline Analysis . . . 13

5 Discussion **13**

5.1 Limitations . . . 13

6 Conclusion and Future Work **14**

6.1 Further Studies . . . 14

A REAL-TIME 3D GUI FOR "SMART SURGICAL GLOVES" WITH LOCATION AND PRESSURE SENSORS

YEAR 3 PROJECT FINAL REPORT

Anthony Chan
Department of Medical Physics and Biomedical Engineering
University College London
London, WC1E 6BT

ABSTRACT

Introduction: The research developed a real-time 3D graphical user interface (GUI) for "Smart Surgical Gloves" equipped with location and pressure sensors. The goal is to assist and train clinicians for digital rectal examination (DRE) by providing quantitative data and 3D graphics for visualisation.

Methodology: The system uses an electromagnetic tracking system (Aurora) for location sensing and a FlexiForce force sensor for pressure data. The GUI is built using Python with Pyglet for the 3D graphics and PyQt for the 2D plots. Stress and strain calculations help analyse the material properties. Prostate phantoms were made with different materials to simulate the DRE scenario for experimenting with this system.

Results: The are three panels: 3D graphics of the hand movement, a stress-against-time graph for monitoring stress, and a stress-strain plot. There is also an offline stress-strain plot for analysing the data from different trials. The 3D graphics provide clear visual feedback during the modelled DRE scenario. The stress plots and stress-strain curves might assist in assessing tissue stiffness. The code and demonstration video can be found on GitHub: `https://github.com/FishBallMEOW/BME-UG-Project-2023-24-Smart-Surgical-Gloves`.

Conclusion: This GUI system could potentially assist the training and diagnostic process for DRE. There are, however, limitations like mobility and clinical significance. Further clinical studies are therefore needed to validate the system's effectiveness.

1 Introduction

Computed tomography (CT), magnetic resonance imaging (MRI) or biopsy would probably be the first several things that came to mind when mentioning the gold standard. Although these diagnostic methods are highly accurate and commonly used by clinicians, they are expensive, time-consuming, and complicated. Extra concerns might also need to be considered, such as ionising radiation for CT or invasion for biopsy. Other more straightforward methods of diagnosis may be preferred. One of these methods would be through physical examination. Examples will be breast examination or prostate examination for the diagnosis of abnormality (i.e., cancer). In this paper, prostate examination will be the main topic to be discussed.

In every eight males, there is one of them will be diagnosed with prostate cancer during his lifetime.[1] Prostate cancer is the 2nd most common type of cancer among men and the 4th among all. There were more than 1.4 million new cases in 2020 worldwide.[2] Digital rectal examination (DRE) is one of the methods for diagnosing prostate cancer. DRE is a physical examination of the prostate. These physical examinations are more affordable and accessible, as mentioned above. However, these kinds of examinations use sensation or, more specifically, palpation of the clinicians. The results are very prone to the bias of the person who conducts the test. This might lead to a higher chance of error and losing reliability and precision.

A wearable device might be a solution to these issues. With sensors and electronics, quantitative variables like forces applied could be given to clinicians and doctors to assist in diagnosing or aiding surgical procedures. For example,

Layard Horsfall et al. introduced a sensorised surgical glove with pressure sensors.[3] By providing real-time force data during surgery, surgeons could reduce the risk of applying excessive force and damaging tissue in the operations.

Furthermore, 3D visualisation (e.g., Virtual reality, Augmented reality) could enhance these methods even more. This is done by providing an intuitive medium to train clinicians or surgeons. A systematic review from T. Joda et al. suggests that 3D visualisation (VR and AR) for dental medicine is receiving increasing interest in education.[4] Apart from education, T. Huang et al. also stated that VR or AR would be useful for assisting physicians in delivering operations with accurate tracking systems and medical images.[5] The reduction of learning difficulties for clinicians could potentially increase the number of clinicians that could conduct the test. More accurate results could also be delivered. All these lead to vast advantages for the population. This motivates this study to develop a 3D real-time visualisation for prostate examination with sensorised surgical gloves, or the "Smart Surgical Gloves".

2 Literature Review

2.1 Current clinical diagnostic approaches

A traditional way of diagnosing prostate cancer will consist of a DRE and prostate-specific antigen (PSA) blood test. Followed by a transrectal ultrasound (TRUS) guided biopsy if needed. [6] There are a few other guidelines used for prostate cancer's clinical diagnostic process. Examples would be NICE (National Institute for Health and Care Excellence)[7] and AUA/SUO (American Urological Association/Society of Urologic Oncology)[8]. But in general, the process could be separated into two main categories: **pre-biopsy screening** and **biopsy**. Research has been working on improving the biopsy process. An example would be using mpMRI-guided biopsy to improve sensitivity [6]. There are, however, some unpleasant complications like blood in the urine, bowel movements, and semen might present after the biopsy.[7] Therefore, it will be crucial to have a pre-screening with high sensitivity and specificity to prevent unnecessary biopsy. There are quite a few of these pre-screening methods. Here are two common examples mentioned previously for the traditional process:

Prostate-Specific Antigen (PSA) blood test PSA is an enzyme found in both normal prostate endothelial cells and prostate cancer cells.[9] The rise in PSA level is used as an indication for biopsy. A high level of PSA with biopsy confirms the diagnosis of prostate cancer.[10]

Digital Rectal Examination (DRE) DRE is a physical examination of the prostate. Clinicians will examine the prostate by pressing the prostate. Prostate cancer is identified with abnormal stiffness in the prostate. Martinez-Vidal et al. suggested that stiffness correlates with the disease's severity.[11] Another study also found the difference in stiffness between normal and cancerous prostate cells and stated stiffness is a promising biomarker overall.[12]

Although both PSA and DRE are recommended by the Canadian Urological Association[13], there are some disagreements in using these methods. Some stated that PSA blood tests have low specificity.[14] One research also reports that there is not enough evidence supporting the effectiveness of DRE and against using it.[15] A study has suggested that this limitation in using DRE might be due to the lack of training and senior supervision.[16] This paper is, therefore, trying to improve DRE by providing quantitative data and a potentially more intuitive way of training clinicians.

2.2 Wearable technology

This enhancement in DRE could be done with wearable technology, which is electronics worn by the user(s). Wearable technology is a broad topic and has been widely used in daily life. Apple Watch is one of the most well-known examples of wearable technology used in everyday life. There are also many other examples, like Virtual Reality (VR) headsets and Augmented Reality (AR) Glasses. Other examples of wearable technology used in the medical field include the Vitalsens VS100 system from Intelesens Ltd. (Northern Ireland). This CE-approved device was evaluated by Harper et al. [17], showing a good correlation with the results taken by the nurse. It also indicates that the device could pick up abnormalities that might be missed with basic observation. This shows the potential of wearable technology as a powerful tool to help in the medical field.

2.3 Related Works

2.3.1 Sensorised Gloves

The hand is the primary tool used by clinicians and surgeons. They wear surgical gloves during examinations or surgeries to protect their hands. Therefore, it doesn't seem odd when pressure and location sensors were decided to

be integrated into surgical gloves. This idea of putting sensors into surgical gloves is not new. There have been a few examples of integrating sensors into surgical gloves: Layard Horsfall et al. introduced a sensorised surgical glove for analysing the force during neurosurgery.[18] In this study, a soft piezoresistive sensor is used to detect force. The real-time force data optimises the force on the tissue during surgery, preventing damage to the tissue. It could also be used for training and assessing clinicians. Another example would be King et al., who developed a wireless sensor glove for assessing surgical skills during laparoscopic surgery. It evaluates the skill using machine learning. Data is collected from the accelerometers and the bend sensor during surgery. Based on these data, the machine learning model will assess the surgeon’s skill. [19] There is also a study that used sensorised surgical gloves with triboelectric sensors to aid in training and detecting obstetric anal sphincter injury.[20] All of these examples use different sensors and are in various cases. However, they have similar purposes for training and evaluating the skills of the clinicians, which is also one of the aims of this study. In addition to that objective, this study also aims to assist the diagnostic process with quantitative data.

2.3.2 3D graphics in medical field

In this study, a 3D GUI will be utilised to visualise the DRE process better. As mentioned in the introduction, there are studies that have been done on applying 3D graphics in some cases other than DRE[4, 5]. They have stated the potential effectiveness of 3D graphics in education and assisting the surgical procedure. A study has also used an augmented system on DRE for training and assessment. The results from the survey in that study have shown that users think it’s useful for training and teaching.[21] The 3D-GUI in this study has similar principles in providing visualisation to users and potentially having the same effect. All of these related studies have provided sufficient proof to support the possible advantages of this 3D-GUI system.

3 Methodology

3.1 Scenario setup and the general structure of the system

This paper will use the Digital Rectal Examination (DRE) procedure as an example of applying the "Smart Surgical Gloves", or the sensorised gloves. There are many other possible applications, such as obstetric examination and clinical breast examination. This system of real-time 3D GUI with sensorised gloves might also apply to these applications. Some settings might need to be varied to adapt to these changes. Going back to the main objective of this study, which is digital rectum examination (DRE). To replicate the DRE scenario, prostate phantoms were made with different materials. The details about these phantoms will be further discussed in section 3.5. These phantoms will be pressed by the experimenter wearing the sensorised gloves. Data from the sensors will be transferred to the computer. The application of GUI visualisation was developed based on these data. In practical situations, these data will be collected in a real-time setup. Going through the data processing, 2D and 3D graphics will be generated in real-time. Data will also be stored for offline graphics and analysis. Figure 1 illustrates the general structure of this system that is just mentioned.

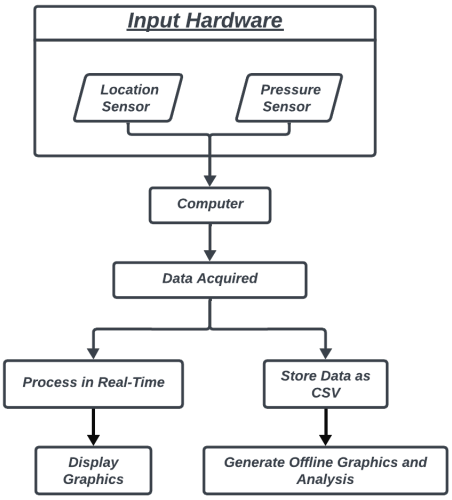

Figure 1: General structure of the system

3.2 Input Hardware

The input hardware is the first layer of the system, as shown in the general structure (Figure 1). The input hardware could be categorised into two sections:

Location Sensor The location sensor used is the NDI Aurora electromagnetic tracking system. This system is visualised in Figure 2. This system consists of four main components (Figure 3a)): The location sensor, the field generator, the sensor interface unit, and the system control unit. The field generator will generate a magnetic field, and the sensor(s) with copper coils in the x,y, and z axes will cut through the field and generate a current. The magnitude of this current could be converted into the movement. The resulting data will be transferred from the system control unit to the computer.

Force Sensor The force sensor is the FlexiForce force sensor (Figure 3b)). The system for the signal conditioning of this sensor was built by Koide and Pernollet last year. This system (Figure 2) comprises a FlexiForce force sensor, a Quicksmart board and an Arduino board. The signal from the sensor will be transferred to the Quicksmart Board for signal conditioning. After that, it will be input into the Arduino.

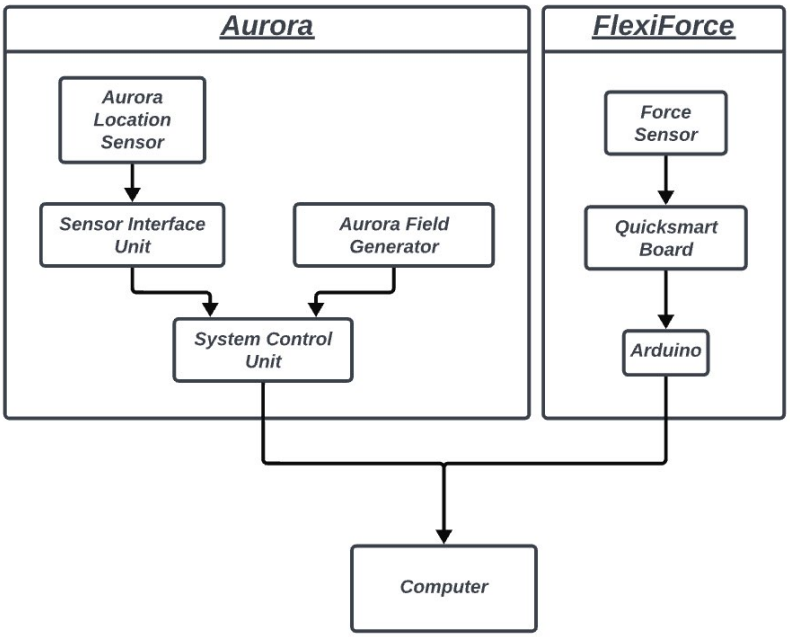

Figure 2: Detailed setups of the location sensor(Aurora) and the force sensor(FlexiForce).

a)

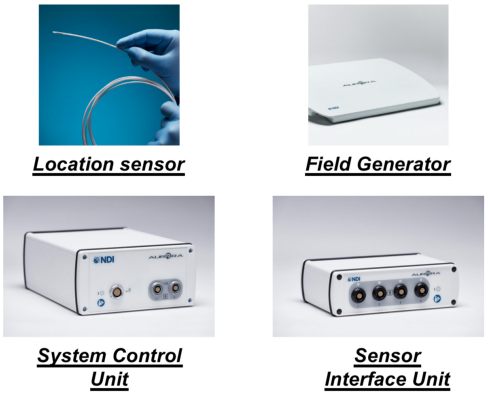

b)

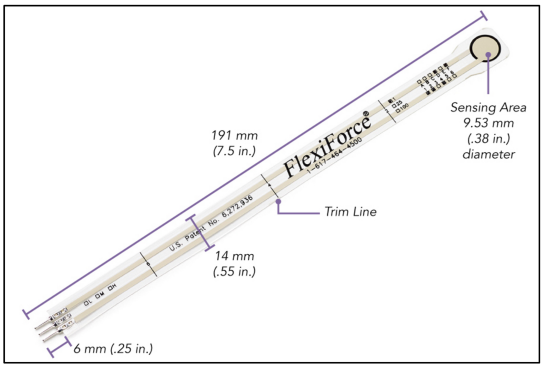

Figure 3: a) Components in the Aurora electromagnetic tracking system.[22] b) the FlexiForce Sensor[23]

3.3 Data acquisition

The data from the input will be input into the computer for further processing. The 3D-GUI system is built in Python, so the first step will be to acquire this data in Python.

3.3.1 Reading the input data

Two libraries from Python will be needed for each signal from the two separate sensors: **SciKit-Surgery** and **Serial**. SciKit-Surgery reads data from the Aurora location tracking system. Serial reads serial data from the Arduino, which is the force data from the Flexiforce force sensor.

3.3.2 Synchronisation

Significant delays in readings were observed in Koide’s work last year. The same equipment has been used for this project. Therefore, the library threading in Python was used to prevent the same issue. In this case, ’Thread’ could be considered the action used to collect sensor data. Therefore, there will be two threads (collecting data from force and location sensors). Typically, each thread could only be executed after finishing the previous one. This might introduce delays. The threading library could prevent this by applying multithreading, which runs multiple sections or ’threads’ concurrently for the code. This concept of multithreading could be visualised through the figure 4. With the aid of this library, the data from the two different sensors could then be collected at almost the same time, reducing the delay. The timestamps of the input data are recorded (figure 5). The difference between the two inputs is around 0.02 seconds. This is not significant.

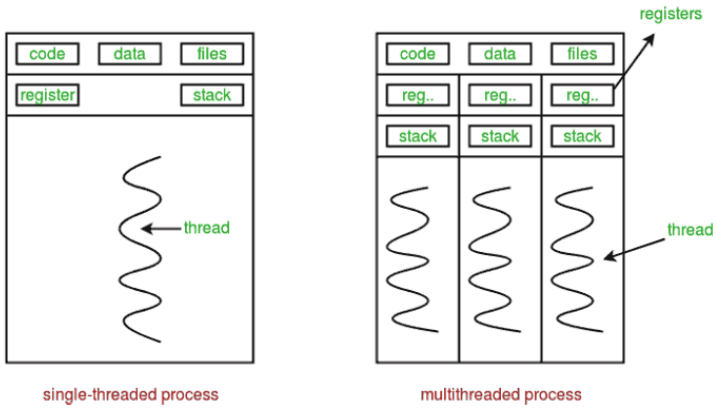

Figure 4: Difference between single-threaded process and multithreaded process [24]

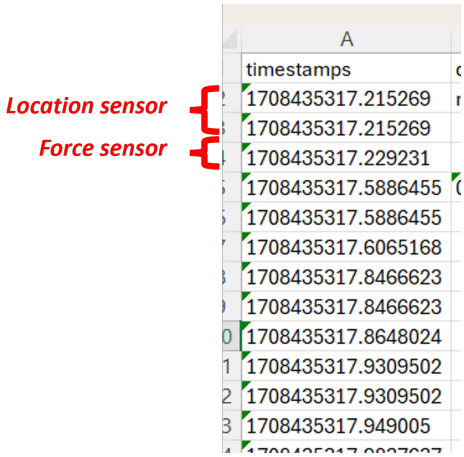

Figure 5: The recorded timestamps of the two inputs (location and force sensors).

3.3.3 Offline simulation

Setting up the tracking system to run the real-time program takes some time. Also, to take a record for the users to revise afterwards, the data will be collected into a CSV file when the real-time program is run. The CSV file could then be used for offline simulation and ease code development. This will save time and allow for more efficient code development.

3.4 Data Processing

3.4.1 Coordinates

The coordinate system of the Aurora magnetic tracking system is different from the coordinate system used in the Pyglet, which uses OpenGL. The perspective mode has been chosen in the Python code. Both coordinate systems are displayed in the figure 6. To visualise the actual location of the sensor correctly in the application, a conversion between these two coordinate systems is needed. The exact formula for converting the coordinates can be found in the code on GitHub.

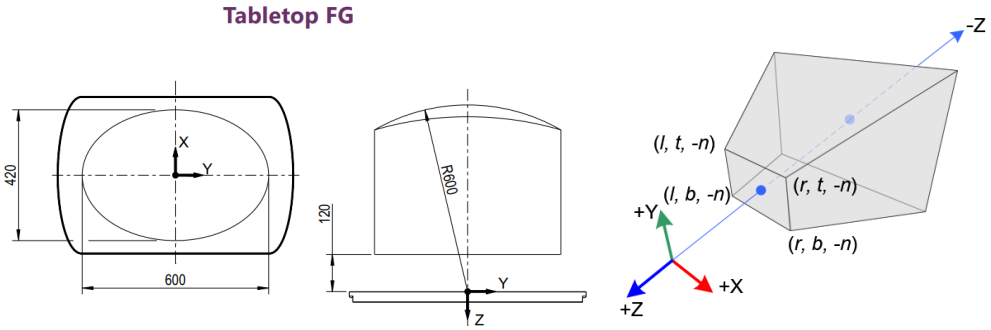

Figure 6: The coordinate system of Aurora[22] (left) and OpenGL[25] (right)

3.4.2 Quaternion and Euler angle

Another issue within the display would be the orientation of the hand/glove. Just like the coordinate systems, there are also two different systems to describe the orientation. Aurora uses quaternion, and OpenGL uses Euler angle (Figure 7). A conversion will, therefore, be needed. As there was a coordinate conversion between the two systems previously, the object's orientation should be set more carefully. The rotation axes should be correctly input into the OpenGL system with the converted axes (i.e., The +z-axis of the OpenGL system is the—x-axis in the Aurora system). Moreover, the order of the rotation matrix multiplication matters, so they must be correctly placed in the code.

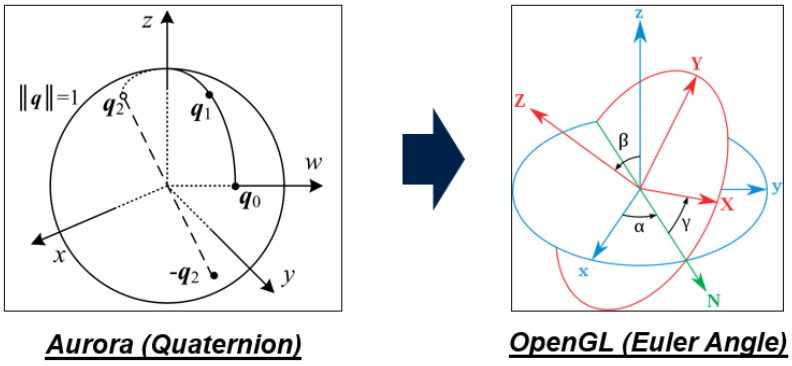

Figure 7: Convert from the Aurora's quaternion to OpenGL's Euler angle.

3.4.3 Stress and Strain

With the location data and force data from the sensors, stress and strain could be calculated for analysing the material property:

Strain The formula for calculating strain:

$$\epsilon = \frac{\Delta L}{L_0} \tag{1}$$

where ϵ is the strain, ΔL is the deformed length, L_0 is the original length. The deformed length will be calculated using the location data. A detailed explanation for this calculation is discussed in Section 3.4.4. A semi-spherical dome-shaped phantom is used, as mentioned in section 3.5. The original length will, therefore, be assumed to be 25mm, which is the radius of the semi-sphere.

Stress The formula for calculating stress:

$$\sigma = \frac{F}{A} \tag{2}$$

where σ is the stress, F is the applied force, A is the area. The applied force is the force data from the flexiforce sensor. The area would be the sensing area of the sensor (Figure 8). This assumes the user is using the entire area of the sensor.

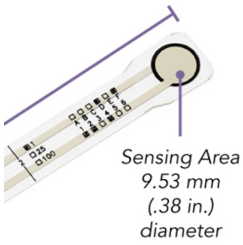

Figure 8: Sensing area of the FlexiForce sensor. [23]

3.4.4 Triggering

Two location points will be needed to calculate the deformation: the initial and current locations. The initial location will be obtained by using triggers. This works by using a start condition and a stopping condition. (Figure 10)

Starting condition The trigger will be turned on when the stress is first over the threshold, which is set to 2kPa (This value is chosen through trial and error). At the time step when the trigger is turned on, it will record that current location point as the initial point and keep it the same until the trigger is off. In the next time step, if the stopping condition is not met, the distance between the current and initial locations will be calculated. This is for the deformation distance for calculating the strain (in section 3.4.3). The calculated stress and stress will only be added to the stress-strain plot if the trigger is on.

Stopping condition The stopping condition is set to be the stress difference $\frac{d\sigma}{dt} <= 0$. This is for the ease of obtaining the stiffness(Young's modulus). The fitting would be easier and more accurate with only the data when the compressive stress rises (Figure 9). After the trigger is turned off, the stored initial location will be reset (Figure 10).

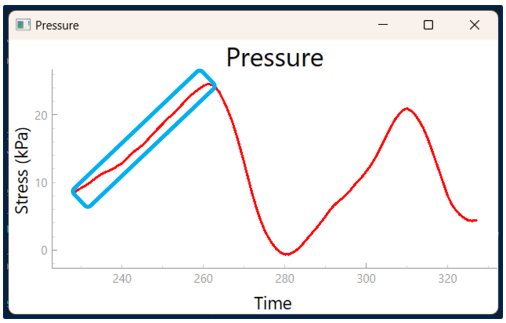

Figure 9: The rising region in the stress data

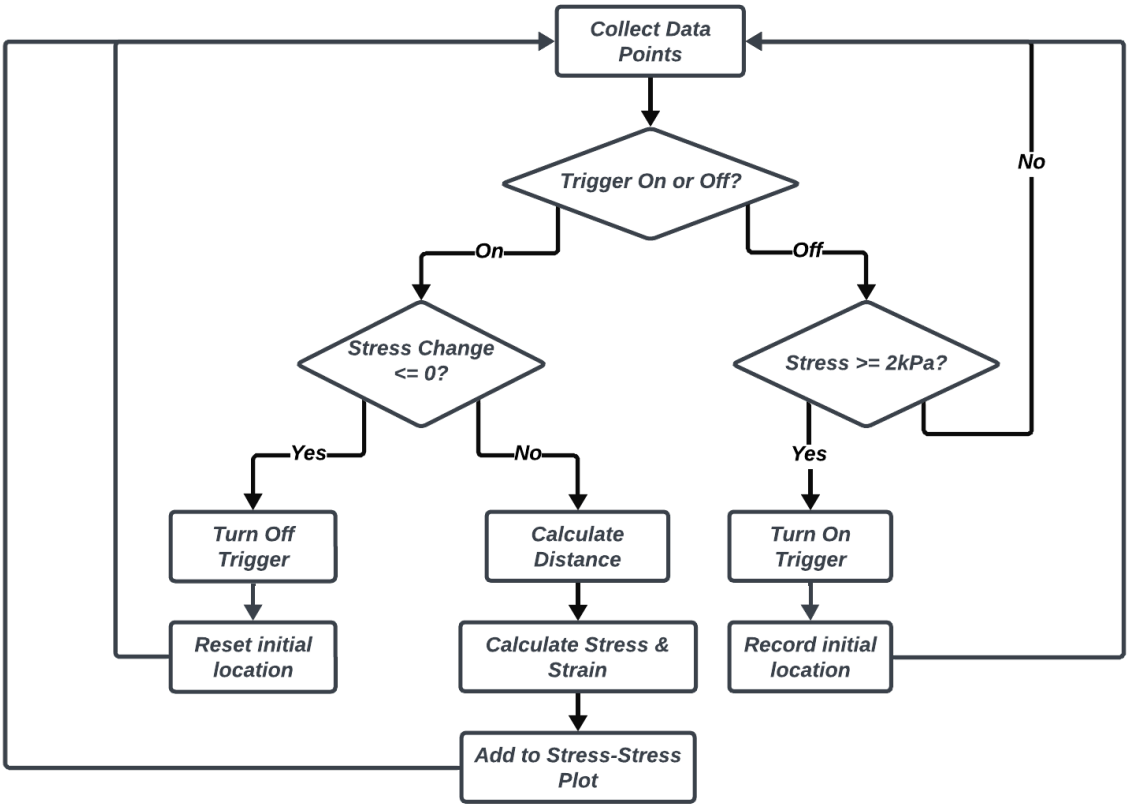

Figure 10: Flowchart displaying the triggering conditions

3.4.5 Moving Average

A technique called moving average is used to reduce the fluctuation of noise observed in the pressure data. This is done by averaging several previous and current data points. Using this average as the new output will smooth the curve, as shown in figure 11. Other than removing the fluctuation, another reason for using this technique is to ensure the curve is smooth for triggering. If there are fluctuations in the stress data, the triggering will keep turning on and off. This led to an earlier change of initial location than it should have, causing the calculation for strain to be inaccurate.

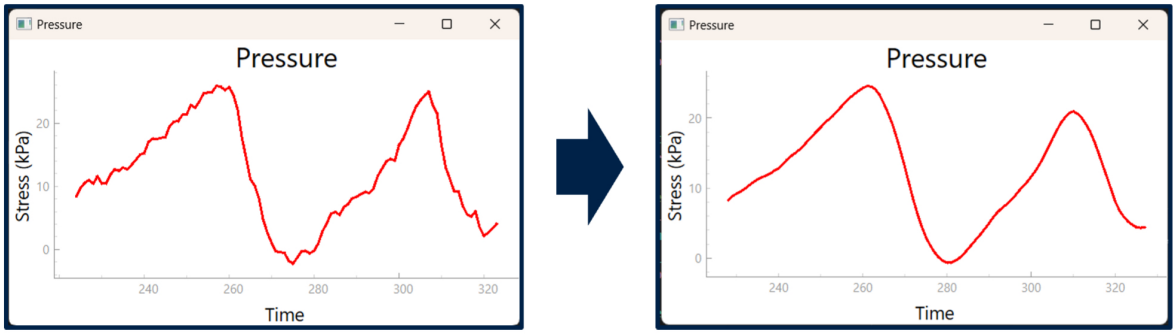

Figure 11: Stress plot before(left) and after(right) using Moving Average

3.4.6 Locating Region

An extra location sensor is used to locate the prostate phantom. The distance between this sensor and the moving sensor will be calculated. With this information, the pressed region of the phantom could be identified (shown in red on the phantom model in Figure 12). This might assist the user in visualising the examination and, more precisely, locating the affected region. There are not many divisions of the model in this study, as shown in Figure 12. The divisions could probably increase with some coding techniques. However, with the limitation of time, this number of divisions would be enough for the purpose of this study.

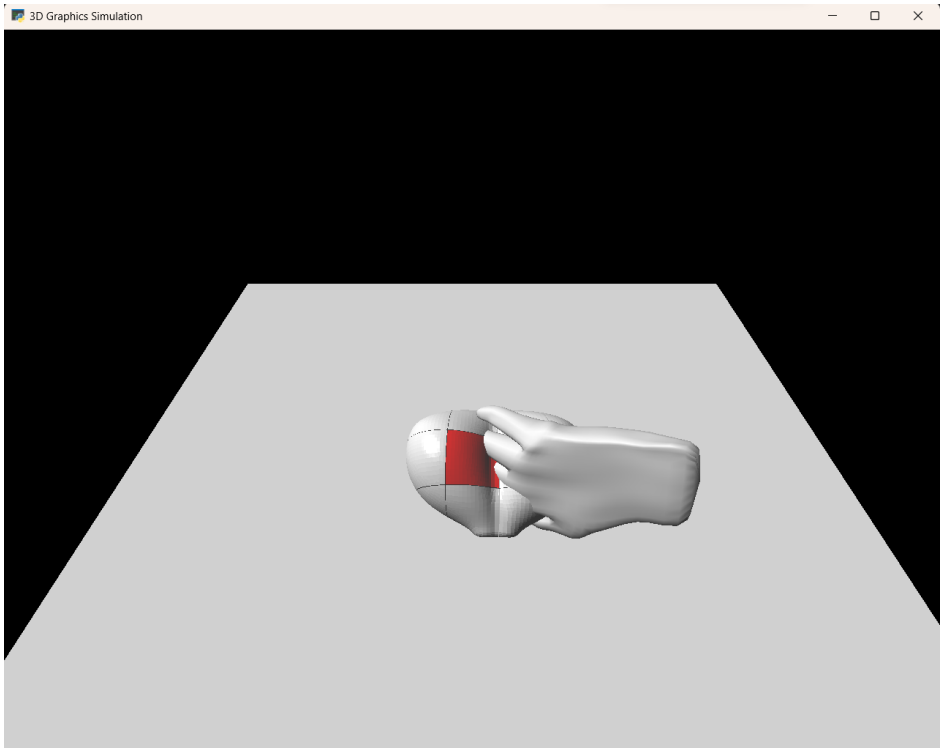

Figure 12: Dividing the phantom model into different sections. Locating the pressed region in red.

3.5 Experiment with phantoms

As there are differences observed between cancerous and normal prostates (as mentioned in section 2.1), phantoms with different stiffness will be used to model this. The phantoms are made with three different materials: EcoFlex 00-10, EcoFlex 00-30, EcoFlex 00-50. The phantoms are made in a semi-sphere dome shape (Figure 13a)). The experimenter will be pressing these phantoms to mimic the process of DRE. Although these phantoms are in dome shape. The phantom models in 3D graphics have a more realistic shape for better visualisation. (Figure 13b))

a) 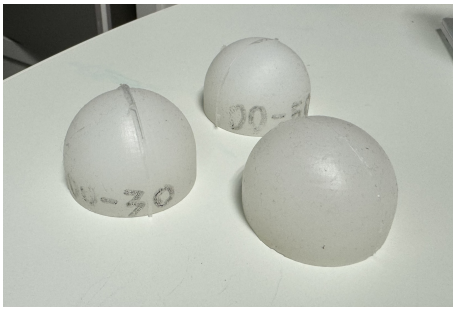 b) 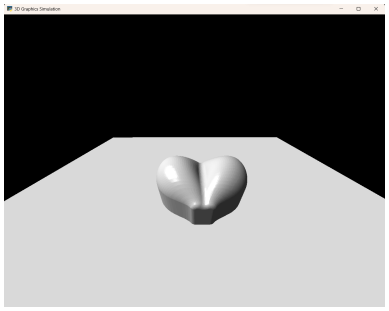

Figure 13: a) The semi-spherical phantoms used for the experiments (made with three different materials). b) The phantom models in 3D graphics.

4 Results

Results in real-time and offline can be found on GitHub: `https://github.com/FishBallMEOW/BME-UG-Project-2023-24-Smart-Surgical-Gloves`

4.1 3D-Graphics

Here is the figure of the 3D-Graphics user interface (Figure 14):

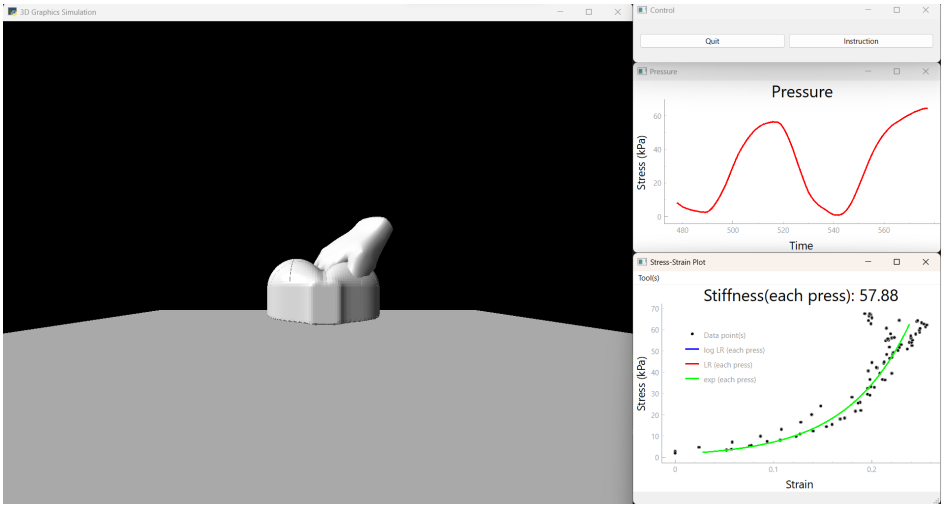

Figure 14: 3D-Graphics user interface

More detailed demonstration videos can be found on GitHub.

4.2 2D-Graphics

A challenge encountered during development is the real-time 2D plots. The library matplotlib was initially used. This is because it is the most commonly used library for plotting in Python. However, after a few trials with matplotlib, it has shown bad real-time performance with a slow frame rate. Even with techniques like blitting used, the frame rate is still very slow at around 3-5 FPS. This drastically slows down the whole program and causes lagging.

Another plotting library, PyQtGraph, was therefore used. Despite being completely written in Python, it is fast as it extensively uses Numpy for number crunching.[26] This significantly increases the frame rate, and the whole program runs smoothly.

4.2.1 Stress plot

A stress plot panel allows the user to monitor the pressure applied to the subject. Here is an example of the plot:

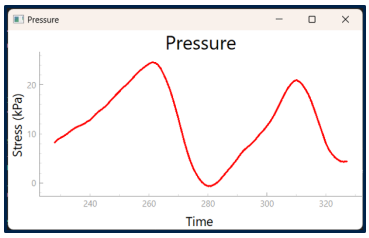

Figure 15: A real-time plot with PyQtGraph

Videos demonstrating the stress plot can also be found on GitHub.

4.2.2 Stress-Strain Plot

Another 2D plot, the stress-strain plot, is provided for the user to analyse the material properties like stiffness. Here are some built-in features to assist the users.

Fitting model A regression line will be plotted according to the stress and strain data. Users could choose from 3 regression models: linear, exponential, and logarithmic (Figure 16a). This regression fitting is done by using the Python library numpy. There will be three formulas for each model:

$$\text{Linear: } y = mx + c \tag{3}$$

$$\text{Exponential: } y = e^{mx+c} \tag{4}$$

$$\text{Logarithmic: } y = m\ln(x) + c \tag{5}$$

By inputting the data and the formula of the chosen fitting model, the coefficients m and c will be outputted in the formula that will fit the data. A curve could then be plotted based on these coefficients and the formula. An example of the fitting curve is displayed in Figure 16b:

Stiffness Stiffness (Young's Modulus) could be calculated by:

$$E = \frac{\sigma}{\epsilon} \tag{6}$$

which is stress divided by strain, which is the gradient of the stress-strain plot. This could be obtained by differentiating the formula obtained after fitting (with the coefficient) and substituting the minimum strain in the data (obtaining the initial gradient). The value of Young's modulus will be displayed in the plot's title as shown in Figure 16c.

Reference values As mentioned in section 2.1, stiffness could be a good biomarker to identify between normal and cancerous prostate. Reference stiffness values of the normal and cancerous prostate at 0.1Hz will be shown at the bottom of the plot Figure 16c. (~3.8kPa for normal and ~7.8kPa for cancerous [12].) This could provide a reference for the user to identify the issues.

Clearing The user could choose to clear just the data points, just the fitting curve, or both of them. (Figure 16d))

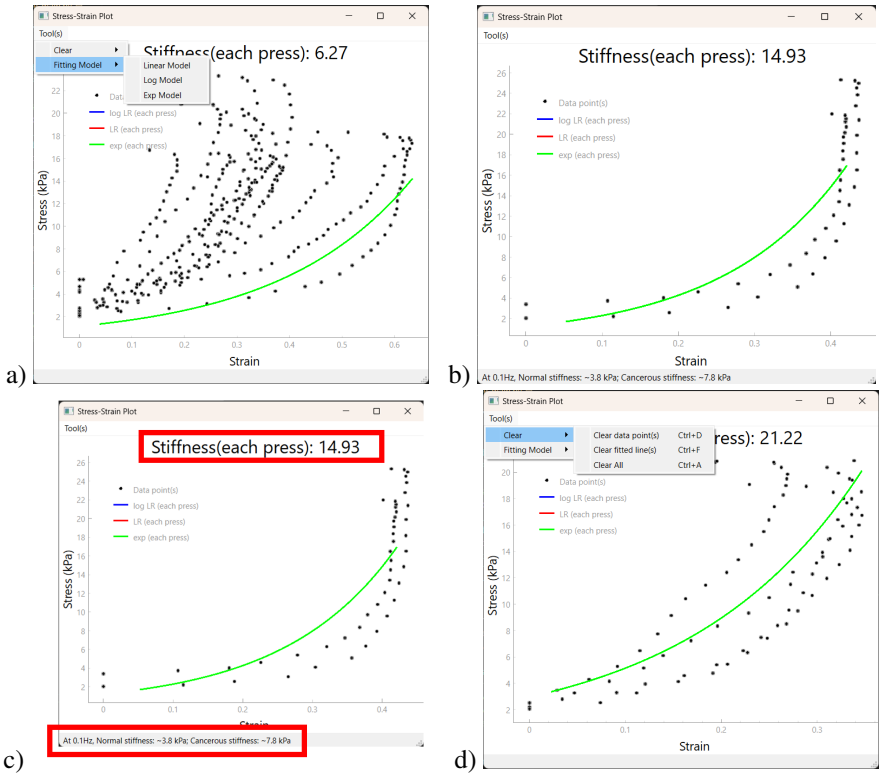

Figure 16: a) Fitting model choices; b) Fitting the data with an exponential curve; c) Calculated stiffness (Young's Modulus) and reference values; d) Clearing choices

4.3 Offline Analysis

A stress-strain plot with all three different materials is drawn offline with Matlab (Figure 17). The figure shows a clear difference between the EcoFlex 00-10 and both EcoFlex 00-30 and EcoFlex 00-50. However, there is an overlap between EcoFlex 00-30 and EcoFlec 00-50. More detailed investigation might be needed to confirm if this system could identify between normal and cancerous prostate tissue. This will be discussed more in the Discussion section (section 5).

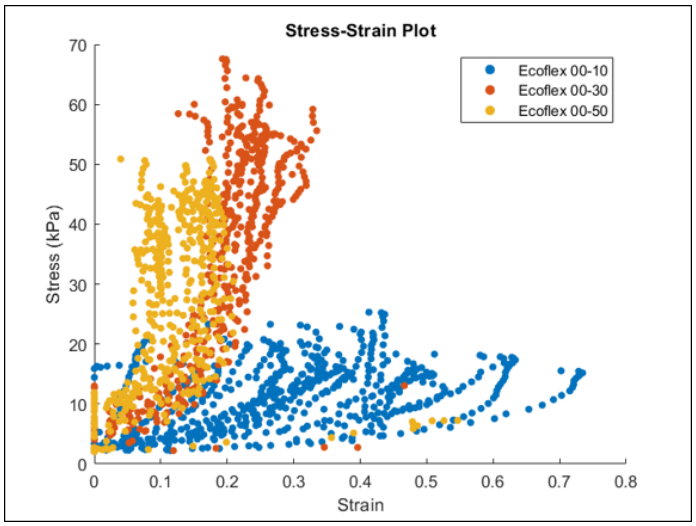

Figure 17: Offline Stress-Strain plot with all three different materials

5 Discussion

The result shows a clear 3D visualisation of the hand movement during the modelled DRE scenario. This visualisation could help the clinicians' training process. The 2D stress-strain plot also potentially aids in diagnosing prostate cancer by providing a metric: stiffness. This might reduce the difficulty of the examination by providing quantitative data. This increases the number of clinicians who can carry out DRE, relieving the pressure on medical resources. Moreover, this system also has the potential to apply to any other physical examination that requires palpation. More research might be needed to adapt to the change, though. However, none of these are supported by any clinical or in vivo study. This study just introduces this system and its potential advantages. This system has other limitations, which will be discussed later in section 5.1. There is still a lot of work and testing to be done in order to launch this system into practical use.

5.1 Limitations

Reference location sensor The reference location sensor could be easily located in the setting with phantoms. This might not be the case in the clinical setting. The sensor might be moved during the examination. A method of fixation will need to be developed. The placing procedure of the reference sensor should also be considered. Some imaging methods might be needed to guide the clinicians. So that they could place the sensor correctly in the location they want. It might need to standardise the location to place the sensor. There are so many complications caused. Therefore, it would be best if there were some alternatives to locate the prostate.

Wireless Both the location and force sensors are now wired to the computer through serial ports. This will limit the mobility of the system. Especially for the location sensor, there is a limited sensing region as it depends on the generated magnetic field.

Clinical significance As seen in the offline stress-strain plot analysis in section 4.3, there are some overlapping data points between different materials. The significance level in distinguishing between normal and cancerous tissues is unknown and needs to be investigated.

Phantom(s) The prostate phantoms currently used for the experiment (section 3.5) are not realistic. The stiffness of the materials is not modelled according to the studies (~3.8kPa for normal and ~7.8kPa for cancerous [12]). The shape of the phantoms is also not realistic.

6 Conclusion and Future Work

This research presents a novel system of sensorised gloves with GUI for DRE. This 3D-GUI system for visualising DRE could be a potentially powerful tool for assisting or training clinicians to examine and diagnose the problems. However, there are still limitations and need further studies to improve, as mentioned in the previous discussion (section 5). Here are some possible further studies to enhance this GUI system with the sensorised gloves.

6.1 Further Studies

Mobility The limitation in mobility has been stated in the previous section. A possible solution would be replacing the electromagnetic field tracking system to system with an accelerometer, gyroscope, and, optionally, magnetometer. Doing so could eliminate the limitation due to the magnetic field. However, this means the reference location sensor will be removed. Another way of locating the prostate will be needed. One possible solution would be adding a small camera to the gloves to locate the prostate and the region being pressed. Data could then be transmitted via wireless methods like Bluetooth instead of serial ports. This makes the whole system to be wireless. Murugan has been working on using Bluetooth to transmit the pressure data.

Clinical studies More clinical studies will be needed to investigate the feasibility of this system. As mentioned in the previous section, the significance of identifying cancerous tissue should be investigated. Furthermore, questionnaire studies should also be done to obtain feedback from the clinicians. Improvements should be made according to this feedback. A design cycle (figure 18) should be followed. The cycle should be continued, and more patches will be needed to improve the users' experience.

Realistic models Apart from clinical studies, another research direction would be to improve the phantom model. More realistic models could be developed to represent the scenario better. For example, soft robotics can be used to make an artificial rectum with the prostate inside for a more realistic scenario, or a more realistic prostate phantom can be built with multiple materials (different stiffness in different regions).

Machine Learning approaches Another possible study that could be conducted is combining the machine learning technique. Research has been done on applying machine learning to the PSA blood test. The stiffness calculated from the stress-strain plot could be a possible new input to the machine-learning model. A pipeline of PSA + DRE with machine learning could then be developed. This could help to determine whether a further biopsy should be done.

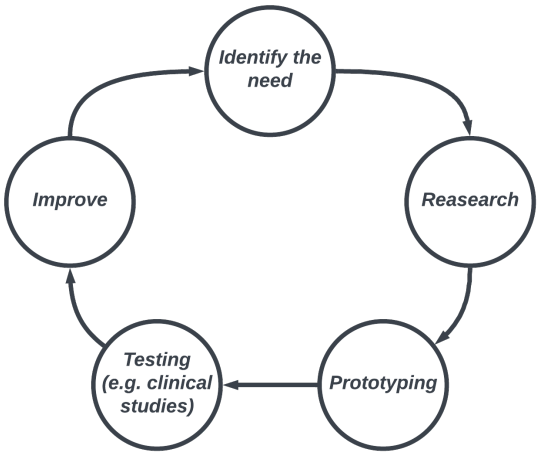

Figure 18: Design Cycle

Acknowledgment

I acknowledge the use of Copilot with GPT-4 Turbo (Microsoft, `https://copilot.microsoft.com/`) to assist in drafting the initial structure of the report, gathering ideas, searching for related works, summarising ideas of some readings, and proofreading my final draft.

I would like to thank my supervisors, Evangelos and Agostino, for giving me this opportunity to work on this project and for their support and insightful feedback during the research.

References

[1] Society AC. Key Statistics for Prostate Cancer | Prostate Cancer Facts; 2024. Available from: https://www.cancer.org/cancer/types/prostate-cancer/about/key-statistics.html.

[2] WCRFI. Prostate cancer statistics | world cancer research fund international; 2020. Available from: https://www.wcrf.org/cancer-trends/prostate-cancer-statistics/.

[3] Layard Horsfall H, Salvadores Fernandez C, Bagchi B, Datta P, Gupta P, Koh CH, et al. A Sensorised Surgical Glove to Analyze Forces During Neurosurgery. Neurosurgery. 2023 03;92:639. Available from: https://journals.lww.com/neurosurgery/Fulltext/2023/03000/A_Sensorised_Surgical_Glove_to_Analyze_Forces.24.aspx.

[4] Joda T, Gallucci GO, Wismeijer D, Zitzmann NU. Augmented and virtual reality in dental medicine: A systematic review. Computers in Biology and Medicine. 2019 05;108:93-100. Available from: https://www.sciencedirect.com/science/article/pii/S001048251930085X.

[5] Huang TK, Yang CH, Hsieh YH, Wang JC, Hung CC. Augmented reality (AR) and virtual reality (VR) applied in dentistry. The Kaohsiung Journal of Medical Sciences. 2018 04;34:243-8.

[6] Descotes JL. Diagnosis of prostate cancer. Asian Journal of Urology. 2019 4;6:129-36.

[7] N. Prostate cancer: diagnosis and management NICE guideline; 2019. Available from: https://www.nice.org.uk/guidance/ng131/resources/prostate-cancer-diagnosis-and-management-pdf-66141714312133.

[8] Wei JT, Barocas D, Carlsson S, Coakley F, Eggener S, Etzioni R, et al. Early Detection of Prostate Cancer: AUA/SUO Guideline Part I: Prostate Cancer Screening. Journal of Urology. 2023 7;210:46-53.

[9] Balk SP, Ko YJ, Bubley GJ. Biology of Prostate-Specific Antigen. 2003. Available from: www.jco.org.

[10] Young GJ, Harrison S, Turner EL, Walsh EI, Oliver SE, Ben-Shlomo Y, et al. Prostate-specific antigen (PSA) testing of men in UK general practice: a 10-year longitudinal cohort study. BMJ Open. 2017 10;7. Available from: /pmc/articles/PMC5665300//pmc/articles/PMC5665300/?report=abstracthttps://www.ncbi.nlm.nih.gov/pmc/articles/PMC5665300/.

[11] Martinez-Vidal L, Murdica V, Venegoni C, Pederzoli F, Bandini M, Necchi A, et al. Causal contributors to tissue stiffness and clinical relevance in urology. Communications Biology 2021 4:1. 2021 8;4:1-16. Available from: https://www.nature.com/articles/s42003-021-02539-7.

[12] Hoyt K, Castaneda B, Zhang M, Nigwekar P, di Sant'Agnese PA, Joseph JV, et al. Tissue elasticity properties as biomarkers for prostate cancer. Cancer biomarkers : section A of Disease markers. 2008;4:213. Available from: /pmc/articles/PMC3144495//pmc/articles/PMC3144495/?report=abstracthttps://www.ncbi.nlm.nih.gov/pmc/articles/PMC3144495/.

[13] Izawa JI, Klotz L, Siemens DR, Kassouf W, So A, Jordan J, et al. Prostate cancer screening: Canadian guidelines 2011. Canadian Urological Association journal = Journal de l'Association des urologues du Canada. 2011 8;5:235-40. Available from: https://pubmed.ncbi.nlm.nih.gov/21801679/.

[14] Merriel SWD, Pocock L, Gilbert E, Creavin S, Walter FM, Spencer A, et al. Systematic review and meta-analysis of the diagnostic accuracy of prostate-specific antigen (PSA) for the detection of prostate cancer in symptomatic patients. BMC Medicine. 2022 12;20:1-11. Available from: https://bmcmedicine.biomedcentral.com/articles/10.1186/s12916-021-02230-y.

[15] Naji L, Randhawa H, Sohani Z, Dennis B, Lautenbach D, Kavanagh O, et al. Digital Rectal Examination for Prostate Cancer Screening in Primary Care: A Systematic Review and Meta-Analysis. The Annals of Family Medicine. 2018 3;16:149-54. Available from: https://www.annfammed.org/content/16/2/149https://www.annfammed.org/content/16/2/149.abstract.

[16] Teoh M, Lee D, Cooke D, Nyandoro MG. Digital Rectal Examination: Perspectives on Current Attitudes, Enablers, and Barriers to Its Performance by Doctors-in-Training. Cureus. 2023 6;15. Available from: /pmc/articles/PMC10278382//pmc/articles/PMC10278382/?report=abstracthttps://www.ncbi.nlm.nih.gov/pmc/articles/PMC10278382/.

[17] Harper R, Donnelly N, McCullough I, Francey J, Anderson J, McLaughlin JA, et al. Evaluation of a CE approved ambulatory patient monitoring device in a general medical ward. 2010 Annual International Conference of the IEEE Engineering in Medicine and Biology Society, EMBC'10. 2010:94-7.

[18] Horsfall HL, Fernandez CS, Bagchi B, Datta P, Gupta P, Koh CH, et al. A Sensorised Surgical Glove to Analyze Forces During Neurosurgery. Neurosurgery. 2023 3;92:639. Available

from: /pmc/articles/PMC10508368//pmc/articles/PMC10508368/?report=abstracthttps://www.ncbi.nlm.nih.gov/pmc/articles/PMC10508368/.

[19] King RC, Atallah L, Lo BPL, Yang GZ. Development of a wireless sensor glove for surgical skills assessment. IEEE Transactions on Information Technology in Biomedicine. 2009;13:673-9.

[20] Jaufuraully SR, Salvadores Fernandez C, Abbas N, Desjardins A, Tiwari MK, David AL, et al. A sensorised surgical glove to improve training and detection of obstetric anal sphincter injury: A pre-clinical study on a pig model. BJOG: An International Journal of Obstetrics Gynaecology. 2024. Available from: https://onlinelibrary.wiley.com/doi/full/10.1111/1471-0528.17762https://onlinelibrary.wiley.com/doi/abs/10.1111/1471-0528.17762https://obgyn.onlinelibrary.wiley.com/doi/10.1111/1471-0528.17762.

[21] Muangpoon T, Osgouei RH, Escobar-Castillejos D, Kontovounisios C, Bello F. Augmented Reality System for Digital Rectal Examination Training and Assessment: System Validation. Journal of Medical Internet Research. 2020 8;22. Available from: /pmc/articles/PMC7453322//pmc/articles/PMC7453322/?report=abstracthttps://www.ncbi.nlm.nih.gov/pmc/articles/PMC7453322/.

[22] Aurora ® Experience new advancements in image-guided surgery and interventional systems with the real-time electromagnetic tracking technology known for its unsurpassed accuracy and ease of integration -the Aurora from NDI;. Available from: https://www.ndieurope.com/wp-content/uploads/2019/11/8300163_rev009_Aurora.pdf.

[23] Sensor FA. FlexiForce A201 Sensor. Tekscan; 2012. Available from: https://www.tekscan.com/products-solutions/force-sensors/a201.

[24] Multithreading in Python | Set 1; 2017. Available from: https://www.geeksforgeeks.org/multithreading-python-set-1/.

[25] Ahn SH. OpenGL Projection Matrix;. Available from: https://www.songho.ca/opengl/gl_projectionmatrix.html.

[26] PyQtGraph - Scientific Graphics and GUI Library for Python;. Available from: https://www.pyqtgraph.org/.